

RESEARCH ARTICLE

# Paradox response of cornea to different color intensities of visible light: An experimental study

Sherif S. Mahmoud<sup>1</sup>\*, Ibrahim H. Ibrahim<sup>2</sup>‡, Abdel Sattar M. Sallam<sup>2</sup>‡, Wafaa A. Gareeb<sup>2</sup>©

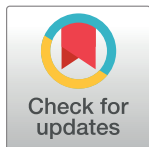
**1** Biophysics and Laser Science Unit, Research Institute of Ophthalmology, Giza, Egypt, Giza, Egypt,

**2** Physics Department, Faculty of Science, Ain Shams University, Cairo, Egypt, Abbasiya Square, Cairo, Egypt

© These authors contributed equally to this work.

‡ These authors also contributed equally to this work.

\* [sheri\\_sm@yahoo.com](mailto:sheri_sm@yahoo.com)



## Abstract

The technological development is associated with human daily life and had an impact on its social life. Due to the difficulty of estimating the daily exposure to light; research is needed to determine how much natural and man-made lights could affect the cornea. Visible light radiation could have damaging effect on the human eye; the type and degree of damage are related to the duration and the cumulative exposure as well as to the intensity of the rays. There are noticeable increases in using electronic devices and colored lamps in decoration and toys as well, without any specific regulation. We studied the effect of such human activity on the corneal structure and the vibrational characteristics of corneal tissue by Fourier transform infrared spectroscopy. To achieve these goals, Chinchilla rabbits were exposed to two different lux of blue, green or red color lamps. The results indicate that the corneal tissue responds non-specifically to each lux and accordingly the color. The detected changes are including corneal protein secondary structure as well as lipids, in particular phospholipids. This was concomitant with more ordered membrane bilayer and changes in the corneal membrane phase organization. No lux/color-response relationship was established.

## OPEN ACCESS

**Citation:** Mahmoud SS, Ibrahim IH, Sallam ASM, Gareeb WA (2018) Paradox response of cornea to different color intensities of visible light: An experimental study. PLoS ONE 13(5): e0196827. <https://doi.org/10.1371/journal.pone.0196827>

**Editor:** Sanjoy Bhattacharya, Bascom Palmer Eye Institute, UNITED STATES

**Received:** September 27, 2017

**Accepted:** April 22, 2018

**Published:** May 25, 2018

**Copyright:** © 2018 Mahmoud et al. This is an open access article distributed under the terms of the [Creative Commons Attribution License](https://creativecommons.org/licenses/by/4.0/), which permits unrestricted use, distribution, and reproduction in any medium, provided the original author and source are credited.

**Data Availability Statement:** All relevant data are within the paper and its Supporting Information files.

**Funding:** The authors received no specific funding for this work.

**Competing interests:** The authors have declared that no competing interests exist.

## Introduction

Human is constantly exposed to a portion of the electromagnetic spectrum where the eye and skin are the primarily target organs [1]. Light is essential for maintaining the circadian rhythm [2] and recently light therapy is included for the treatment of seasonal affective disorder [3]. In addition to the medical applications of optical instruments used in ophthalmic examination, light is used for decoration purposes whether indoor or outdoor. Despite of the risk of exposure to visible light, but without it also has its risk. Phototoxicity of different visible light segments is well known [4–5], and it focuses on the retina with minor attention to the cornea. With the technological evolution, which includes devices such as smart phones and tablets, human life has become closely linked with this technology and, since it is difficult to quantify

light exposure through everyday life, this study is devoted to clarify the possible interaction of corneal structural constituents with different light colors (wavelengths)/lux by recording and analyzing the vibrational characteristics using Fourier transform infrared spectroscopy (FTIR).

## Materials and methods

Healthy Chinchilla rabbits weighing 2.5–3 kg were purchased from the holding company for biological products and vaccine, Cairo, Egypt. Rabbits were fed a balanced diet and received water *ad-libitum*. Use of animals in this study was in compliance with the ARVO statement for the Use of Animals in Ophthalmic and Vision Research, the study was also approved by the Research Institute of Ophthalmology ethical committee (RIO—ethical committee). For irradiation purpose, animals were carefully removed from cages in order to avoid excitement. The potassium bromide-FTIR grade (KBr) powder was purchased from sigma-aldrich (Sigma-Aldrich Co. LLC).

## Visible light exposure

Incandescent lamps (220 V and 60 W) commercially available in the markets were used in this study. Three light lamps (sources) that emit visible light in the blue, green and red regions were calibrated in the National Institute for Standards (Giza, Egypt) in order to determine their illuminance at 10 cm (High lux, H) and 1 m (Low lux, L). The blue lamp ( $\lambda_{\max} = 415$  nm) low lux was 80 (blue-L) and the high lux was 3560 (blue-H). For the green source ( $\lambda_{\max} = 510$  nm) it was 183 (green-L) and 4780 (green-H) lux respectively. The red source ( $\lambda_{\max} = 610$  nm) lux was 162 (red-L) at 1m and 5050 (red-H) at 10 cm. The uncertainty in the measured illumination is  $\pm 3\%$ .

For irradiation purpose, animals were carefully placed in animal's cages so that their heads are exposed. Before irradiation, the eyes were anesthetized by few drops of benox eye drops while the whole rabbits were anesthetized by injection with 0.1 ml/kg separine as muscle relaxant firstly and after 15 min, 0.5 ml/kg ketamine hydrochloride was administered intramuscular. The animal's eye was kept opened during the irradiation using speculum. The light source was adjusted to irradiate the eye by using an obstacle with a hole that was adjusted to fit the diameter of the eye. The thermal effect of light on the exposed eyes was avoided by using infrared filters and water filter, as well as the ambient temperature was set to 20 °C.

Rabbits ( $n = 60$ ) were categorized into six light-irradiated groups each composed of 10 rabbits; one eye was exposed to either low or high lux of the blue, green or red sources while, the contra-lateral eye was used as control. The exposure time for all lux was 60 min/session and repeated three times daily and lasts for one week.

## Fourier transform infrared spectroscopy

After exposure, eyes were enucleated from the globe and corneas were removed by cutting through the ora serrata. Each cornea was crushed into powder in liquid nitrogen and mortar. The resulted corneal powder was then mixed with KBr powder (10 mg:90 mg) and pressed with the instrument-provided pressing kit to prepare the KBr disks that will be used for the FTIR analysis.

Infrared spectra were recorded using Nicolet iS5 FTIR Spectrometer (Thermo Scientific, USA) equipped with TGS detector. The spectra were taken at  $4.0\text{ cm}^{-1}$  resolution at physiological temperature. To avoid the influence of atmospheric  $\text{CO}_2$  and water vapor (if any), the instrument was operated under continuous flow of  $\text{N}_2$  gas. Generally, 100 scans were accumulated to enhance the signal to noise ratio. These interferograms were averaged to produce a

representative group spectrum that was analyzed using OriginPro 7.5 software (Origin Lab Corporation, Northampton, MA, USA).

### Statistical analysis

Data were represented by the mean  $\pm$  SD. In this study the analysis of variance (one way-ANOVA) was used to determine the statistical significance between multiple groups at a significance level of  $p < 0.05$ .

## Results

Infrared spectral analysis will be performed in the following ranges; 4000–3000  $\text{cm}^{-1}$  (amide A and B as well as OH stretching region), 3000–2800  $\text{cm}^{-1}$  (CH stretching region), 1700–1600  $\text{cm}^{-1}$  (amide I region) and 1500–1200  $\text{cm}^{-1}$  (fingerprint region).

### NH-OH stretching region

The NH-OH region of the corneas that includes Amide A ( $_{\text{asym}}\text{NH}$ ) and Amide B ( $_{\text{sym}}\text{NH}$ ) bands is shown in Fig 1. Regarding the main band, the vibrational frequency of control group was found to be  $3434 \pm 1 \text{ cm}^{-1}$ . After the exposure to light sources, two observations can be noticed: the vibrational frequency was increased due to the exposure to low lux (average,  $3446 \pm 5 \text{ cm}^{-1}$ ) and remains unchanged after the exposure to high lux (average,  $3434 \pm 2 \text{ cm}^{-1}$ ) as compared to the control one. The contour of the main band was resolved to its underlying peaks using the curve enhancement-Fourier deconvolution procedure. As shown in Fig 1 and given in Table 1, the number of estimated peaks was decreased after exposure to both low and high lux. The pattern associated with the high lux of the green light (green-H) has the same characteristics as that associated with red-L and red-H; and were characterized by restricted NH stretching vibrational modes as well as the  $_{\text{str}}\text{OH}$  one. Table 1 also indicates that Amide A and Amide B bands were dramatically affected by the exposure to different wavelength/lux; Amide A was restricted in all lux but blue-L where its vibrational frequency was significantly decreased and its bandwidth was increased. On the other hand, Amide B band was restricted in all lux but green-L. The band characteristics of the green-L show significant increase in both frequency and bandwidth.

The OH stretching modes ( $_{\text{asym}}\text{OH}$  and  $_{\text{sym}}\text{OH}$ ) have the same characteristics after the exposure to all lux but blue-L. Its vibrational frequency was decreased concomitant with increased bandwidth as compared to the normal. The other OH vibrational mode ( $_{\text{str}}\text{OH}$ ) was restricted as a result of exposure to green-L, red-L and red-H. The  $_{\text{str}}\text{OH}$  vibrational frequency and its corresponding bandwidth were changed due to exposure to blue-L, blue-H and green-L.

### CH stretching region

Fig 2 and Table 2 summarize the vibrational characteristics of the CH stretching region in the wavenumber range 3000–2800  $\text{cm}^{-1}$ . The normal profile indicates the presence of three bands that discernible at 2960  $\text{cm}^{-1}$  ( $_{\text{asym}}\text{CH}_3$ ), 2923  $\text{cm}^{-1}$  ( $_{\text{asym}}\text{CH}_2$ ) and 2850  $\text{cm}^{-1}$  ( $_{\text{sym}}\text{CH}$ ). For  $_{\text{asym}}\text{CH}_3$  mode of vibration, its vibrational frequency was decreased for high lux exposure concomitant with increased vibrational motion for both low and high lux. In the same context, the vibrational frequency of  $_{\text{asym}}\text{CH}_2$  band was decreased relative to the normal one after the exposure to different light lux. The other observation concerning this band is the increased bandwidth that was associated with low lux only.

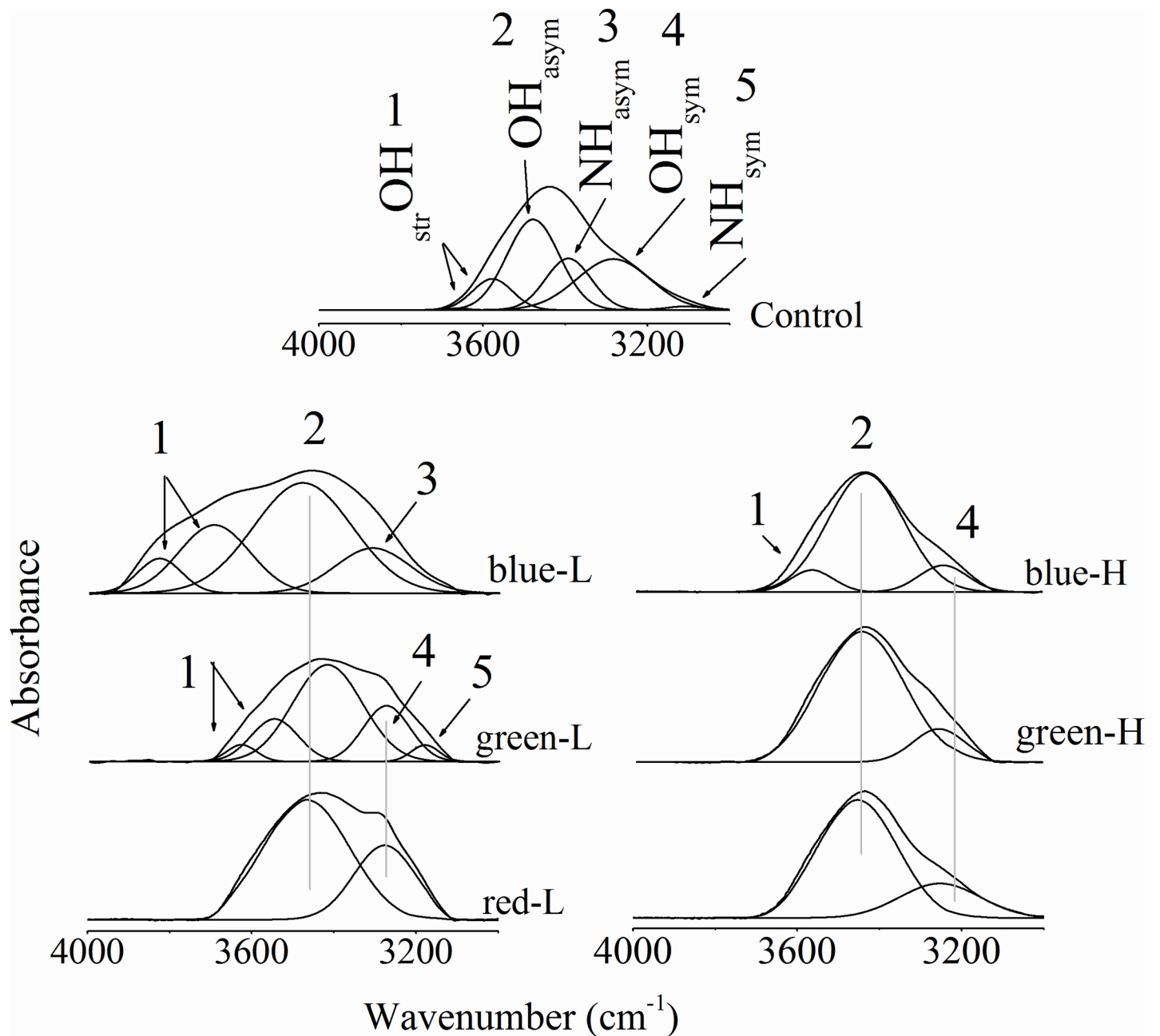


Fig 1. The main NH-OH band and its underlying peaks due to exposure to different color intensities.

<https://doi.org/10.1371/journal.pone.0196827.g001>

The detected  $_{\text{sym}}\text{CH}$  vibrational modes have no changes in their frequency while their bandwidth was changed. The curve enhancement procedure used in this study, resolved the stretching band that noticed in the normal pattern nearly at  $2851\text{ cm}^{-1}$  into two underlying component bands due to exposure to red-L, green-H and red-H. These two bands are centered at  $2860\text{ cm}^{-1}$  and  $2845\text{ cm}^{-1}$  and correspond to  $_{\text{sym}}\text{CH}_3$  and  $_{\text{sym}}\text{CH}_2$  respectively.

### Amide I region

The most sensitive spectral region to protein secondary structural components is the amide I band ( $1700\text{--}1600\text{ cm}^{-1}$ ), which is due almost entirely to  $\text{C}=\text{O}$  stretching vibrations of the

**Table 1. Underlying peaks detected in the NH-OH stretching region showing their vibrational frequency (cm<sup>-1</sup>) and bandwidth (cm<sup>-1</sup>).**

|         | (1)<br>StrOH |           | (2)<br>OH <sub>asym</sub> | (3)<br>Amide A | (4)<br>OH <sub>sym</sub> | (5)<br>Amide B |
|---------|--------------|-----------|---------------------------|----------------|--------------------------|----------------|
| Control |              | 3662 ± 3  | 3577 ± 3                  | 3478 ± 2       | 3362 ± 2                 | 3283 ± 1       |
|         |              | 10 ± 3    | 31 ± 6                    | 116 ± 5        | 58 ± 5                   | 92 ± 4         |
| Blue-L  | 3828 ± 2     | †3695 ± 3 |                           | 3479 ± 2       | †3309 ± 2                |                |
|         | 105 ± 3      | †172 ± 10 |                           | †239 ± 7       | †182 ± 9                 |                |
| Blue-H  |              |           | †3567 ± 1                 | †3435 ± 1      |                          | †3244 ± 1      |
|         |              |           | †104 ± 2                  | †185 ± 5       |                          | †118 ± 7       |
| Green-L |              | †3629 ± 3 | †3548 ± 3                 | †3419 ± 2      |                          | †3276 ± 1      |
|         |              | †71 ± 5   | †113 ± 3                  | †168 ± 5       |                          | †123 ± 9       |
| Green-H |              |           |                           | †3445 ± 1      |                          | 3255 ± 2       |
|         |              |           |                           | †210 ± 8       |                          | †127 ± 2       |
| Red-L   |              |           |                           | †3467 ± 2      |                          | †3276 ± 2      |
|         |              |           |                           | †213 ± 2       |                          | †150 ± 2       |
| Red-H   |              |           |                           | †3453 ± 1      |                          | †3252 ± 3      |
|         |              |           |                           | †197 ± 6       |                          | †194 ± 4       |

†Statistically significant.

In each cell, the first line represents the frequency and the second line reflects the bandwidth.

<https://doi.org/10.1371/journal.pone.0196827.t001>

peptide linkages [6–8]. Fig 3 shows that the contour of the control amide I band was resolved by the curve enhancement procedure into four component bands that centered around 1679 cm<sup>-1</sup> (β-turns), 1656 cm<sup>-1</sup> (α-helix) and two bands at 1630 cm<sup>-1</sup> and 1617 cm<sup>-1</sup> that correspond to β-sheet structures. Exposure to low lux of different colors was associated by increased number of the underlying structural bands in the amide I region. Regarding the low lux of the blue light; there are two β-turns structural components with a total area percentage of 27.6% (relatively higher than the normal content, 4.8%) concomitant with the presence of random coil band at 1644 cm<sup>-1</sup> (17.8%). The α-helix content was markedly decreased from 66.5% in the control pattern to 24.1%. No change in the content of β-sheet was observed. Also the low-lux of the green light induce marked changes in the corneal protein amide I region, there are five structural components that indicates the presence of α-helix (19.2%), β-sheet (54.2%) and β-turns (26.6%). It is clear that the content of α-helix was reduced and both β-sheet and β-turns content were increased. The remarked changes was noticed after the exposure to the low lux of the red light where there are eight secondary structural bands were estimated and reflect the presence of β-turns (17.7%), turns (14.9%), α-helix (15.4%), random coil (14.9%) and three bands corresponds to β-sheet structure (37.1%).

The corneal protein secondary structure components were differing after the exposure to high lux of different light colors. For the blue-H, there are five structural bands and also the α-helix content was reduced (57.9%) concomitant with increased β-sheet content (41.1%) and random coil structure was detected (1%). As a result of exposing the cornea to green-H, the amide I pattern is greatly affected, the α-helical structure is dominant (84%) and β-sheet content was reduced (11%), there is no change in the content of β-turns structure, but the turns structure was detected with an area percentage of 1.3%. High lux of the red color resulted in three structural bands in the amide I region that only represent α-helix (68.9%) and β-sheet (31.3%) structures as given in Table 3.

The detected changes in protein secondary structure so far are not only due to the variation in the individual proportions but also due to hydrogen bonding. As shown in Fig 3, the extended β-sheets (C = O out of phase, 1630 cm<sup>-1</sup>) and the antiparallel β-sheets (1610–1616

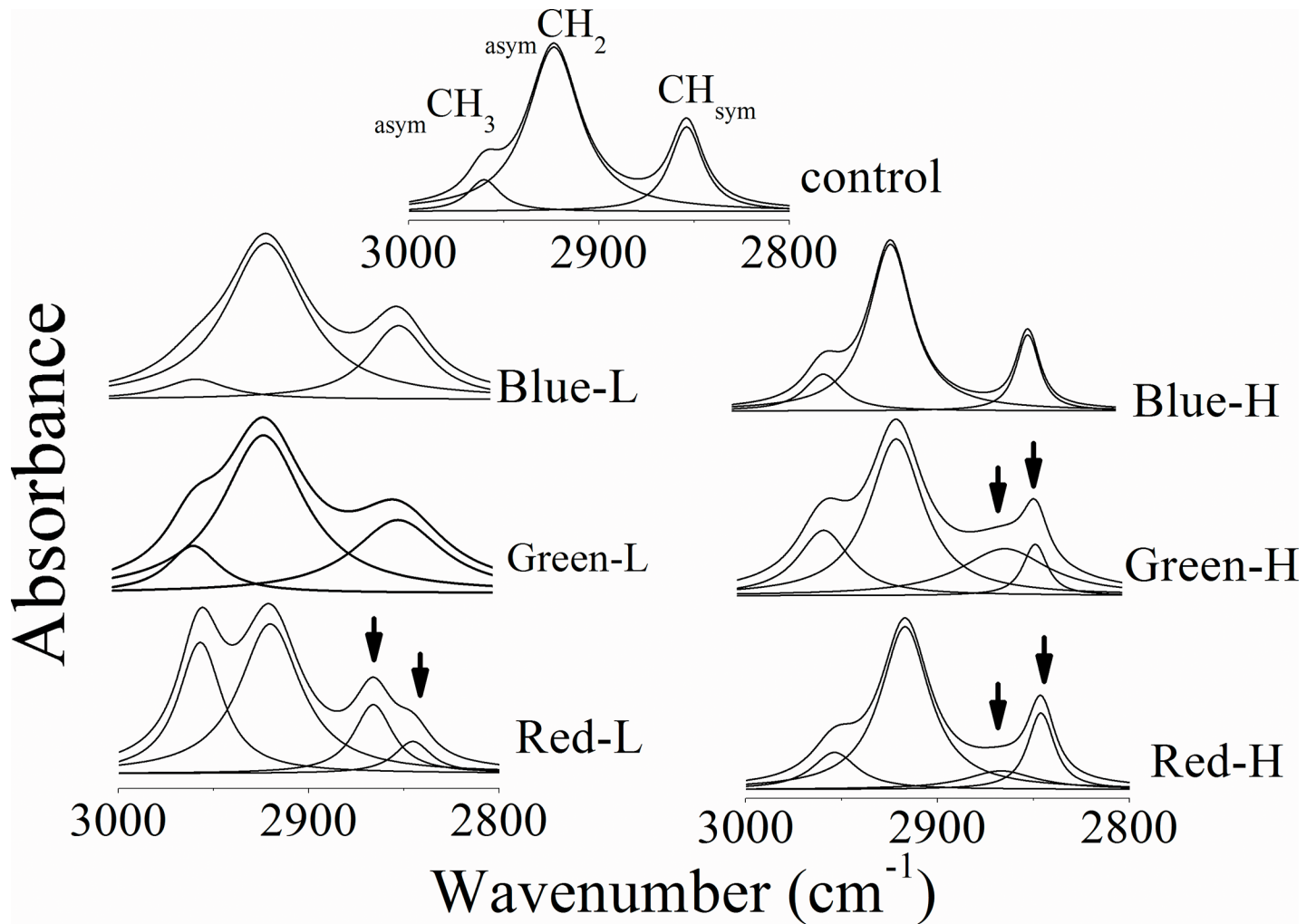


Fig 2. Corneas CH stretching region. Arrows are pointing to the splitting of  $CH_{sym}$  mode into  $symCH_3$  and  $symCH_2$ .

<https://doi.org/10.1371/journal.pone.0196827.g002>

Table 2. Analysis of the CH region showing the underlying peaks vibrational frequency ( $cm^{-1}$ ) and the corresponding bandwidth ( $cm^{-1}$ ).

|            | Control | Blue    |         | Green   |         | Red     |         |
|------------|---------|---------|---------|---------|---------|---------|---------|
|            |         | Low     | High    | Low     | High    | Low     | High    |
| $asymCH_3$ | 2960±3  | 2955±2  | †2952±2 | 2957±2  | †2955±1 | 2957±2  | †2953±1 |
|            | 18±2    | †40±3   | †25±2   | †32±8   | †32±4   | †29±3   | †28±2   |
| $asymCH_2$ | 2925±1  | †2918±2 | †2919±2 | †2920±1 | †2918±2 | †2920±2 | †2918±2 |
|            | 30±4    | †51±4   | 28±4    | †52±5   | 34±3    | †41±5   | 30±3    |
| $symCH$    | 2851±2  | 2849±3  | 2848±3  | 2850±2  |         |         |         |
|            | 20±5    | †38±5   | †13±4   | †57±2   |         |         |         |
| $symCH_3$  |         |         |         |         | 2861±2  | 2866±2  | 2867±1  |
|            |         |         |         |         | 56±8    | 24±9    | 44±6    |
| $symCH_2$  |         |         |         |         | 2845±1  | 2845±1  | 2846±1  |
|            |         |         |         |         | 14±3    | 23±2    | 15±6    |

†Statistically significant.

In each cell, the first line represents the frequency and the second line reflects the bandwidth.

<https://doi.org/10.1371/journal.pone.0196827.t002>

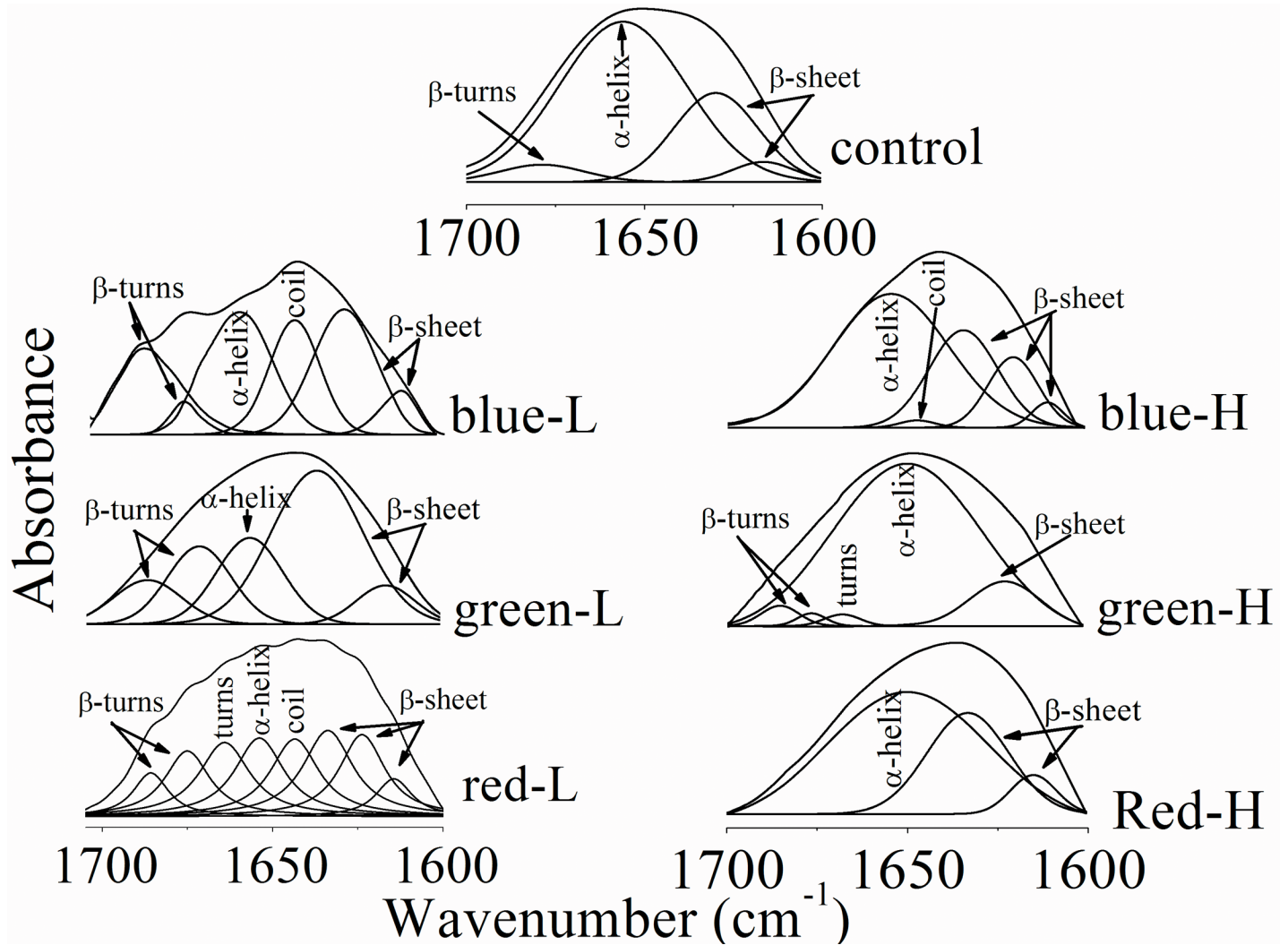


Fig 3. Protein secondary structure components of corneas after exposure to different color intensities.

<https://doi.org/10.1371/journal.pone.0196827.g003>

cm<sup>-1</sup>) are detected in all exposed groups to low and high lux. The changes in the protein secondary structure of the red-L group were associated with the formation of extremely strong

Table 3. The area percentage of protein secondary structure components due to exposure to different wavelength/lux.

|         | Control  | Blue      |           | Green     |         | Red       |          |
|---------|----------|-----------|-----------|-----------|---------|-----------|----------|
|         |          | Low       | High      | Low       | High    | Low       | High     |
| α-helix | 66.5±3.2 | †24.1±1.6 | †57.9±2.6 | †19.2±2.1 | †84±4.4 | †15.4±3.0 | 68.8±1.8 |
| β-sheet | 28.7±4.1 | 30.5±3.7  | †41.1±2.8 | †54.2±4.7 | †11±3.9 | †37.1±1.7 | 31.1±2.4 |
| β-turns | 4.8±1.3  | †27.6±1.8 |           | †26.6±4.1 | 3.7±1.6 | †17.7±1.0 |          |
| Turns   |          |           |           |           | 1.3±0.4 | 14.9±0.6  |          |
| Coil    |          | 17.8±2.5  | 1±0.04    |           |         | 14.9±0.8  |          |

†Statistically significant.

In each cell, the first line represents the frequency and the second line reflects the bandwidth.

<https://doi.org/10.1371/journal.pone.0196827.t003>

intramolecular hydrogen bonding and/or unusual  $\beta$ -sheet structure (underlying peak at  $1625\text{ cm}^{-1}$ ) in addition to parallel  $\beta$ -sheet. This strong hydrogen bonding is evident also in the blue-H exposed group. On contrary, green-H exposed group showed another different variation that is no extended-chain  $\beta$ -sheets.

### Fingerprint bending region

In Fig 4, the fingerprint region ( $1600\text{--}1200\text{ cm}^{-1}$ ) and for amide II band (bending NH); the detected bands in low lux as well as green-H were characterized by reduced vibrational frequency without any change in its vibrational motion. This vibrational mode was undetected due to exposure to blue-H or red-H. On the other hand, the vibrational frequency of the  $\text{CH}_2$  bending band was greatly affected by the exposure to all low or high lux of different light colors involved in this study. In addition to this, cornea- $\text{CH}_2$  bending band was split into two component bands that were centered at  $1458 \pm 1\text{ cm}^{-1}$  and  $1418 \pm 3\text{ cm}^{-1}$  due to exposure to blue-H

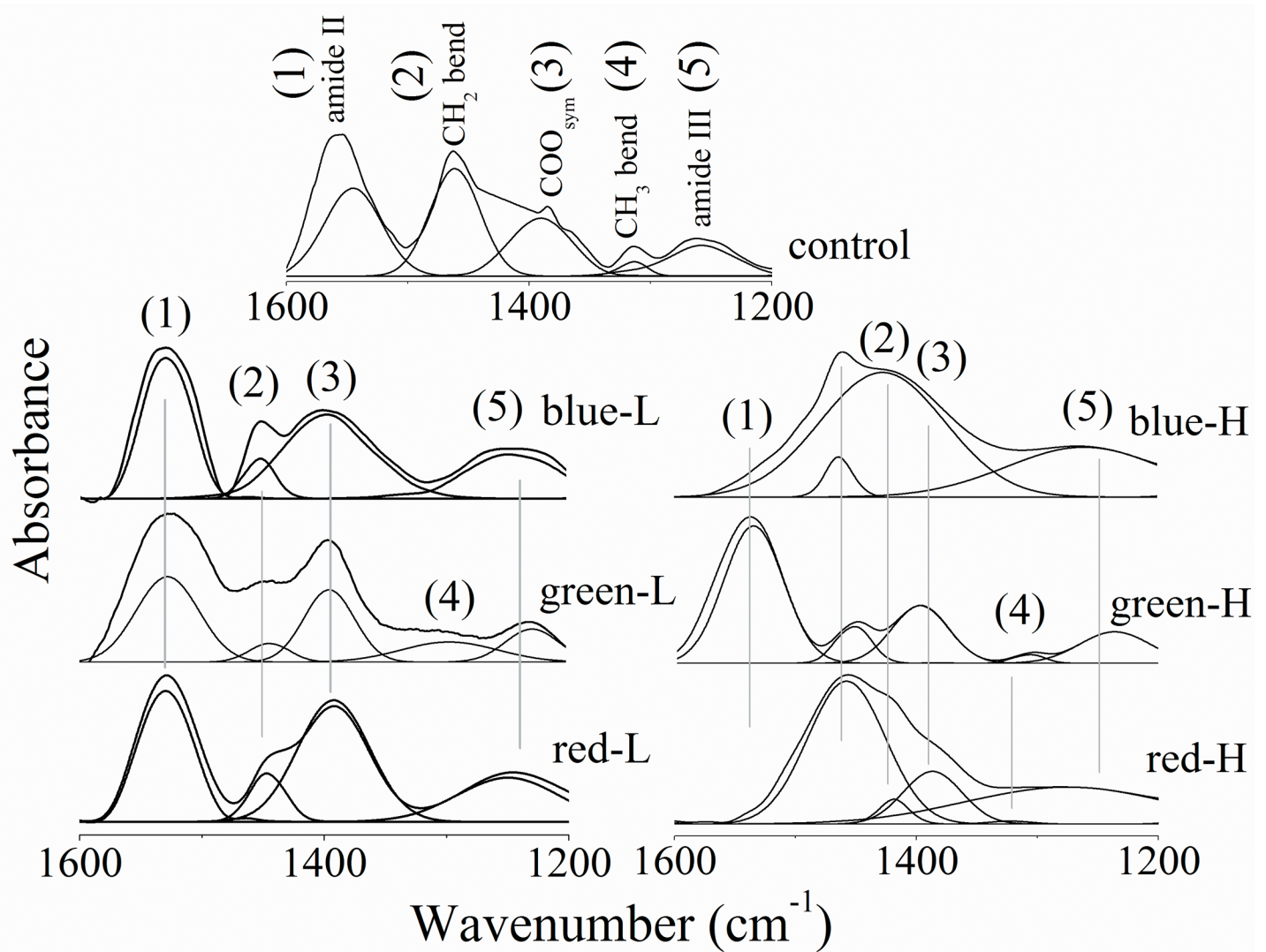


Fig 4. Fingerprint vibrations of corneas from all studied groups showing the underlying peaks.

<https://doi.org/10.1371/journal.pone.0196827.g004>



**Table 4. Fingerprint region showing the bending modes of different bands and their characteristic vibrational frequency (cm<sup>-1</sup>) and bandwidth (cm<sup>-1</sup>).**

|                      | Control | Blue    |        | Green   |         | Red     |         |         |        |
|----------------------|---------|---------|--------|---------|---------|---------|---------|---------|--------|
|                      |         | Low     | High   | Low     | High    | Low     | High    |         |        |
| Amide II             | 1545±1  | †1529±1 |        | †1527±3 | †1536±1 | †1530±2 |         |         |        |
|                      | 44±5    | 44±3    |        | 54±6    | 46±9    | 49±8    |         |         |        |
| bend CH <sub>2</sub> | 1461±2  | †1453±2 | 1463±3 | 1427±3  | †1443±2 | †1453±1 | †1446±2 | 1458±1  | 1418±3 |
|                      | 38±2    | †20±5   | †17±3  | 102±5   | †28±3   | †23±4   | †24±3   | †62±2   | 19±2   |
| symCOO               | 1390±3  | 1395±2  |        |         | 1394±3  | 1396±3  | 1392±3  | 1387±2  |        |
|                      | 53±2    | †75±8   |        |         | †41±4   | †45±1   | 56±2    | †46±2   |        |
| bend CH <sub>3</sub> | 1315±1  |         |        |         | †1296±2 | †1308±2 |         | †1323±2 |        |
|                      | 16±3    |         |        |         | †78±8   | 18±4    |         | †31±6   |        |
| asymPO <sub>2</sub>  | 1258±2  | †1244±1 | 1260±2 |         | †1228±2 | †1236±1 | †1250±2 | †1275±3 |        |
|                      | 69±3    | †85±2   | †128±6 |         | †41±7   | †56±2   | †81±4   | †167±4  |        |

†Statistically significant.

In each cell, the first line represents the frequency and the second line reflects the bandwidth.

<https://doi.org/10.1371/journal.pone.0196827.t004>

and red-H. In the same context, the bandwidth of the CH<sub>2</sub> bending band was markedly changed.

No change in the band position of the symCOO band following the exposure to low or high lux of different light colors. The main observation concerning this band is its disappearance that following the exposure to blue-H. The bandwidth showed many specific characteristics due to the exposure to low lux; increased for blue-L, decreased for green-L and unchanged for red-L (Table 4). The CH<sub>3</sub> bending band was noticed only after the exposure to green light (low or high lux) with reduced band position and after the exposure to red-H (with increased band position and bandwidth) as shown in Table 4.

Finally, asymPO<sub>2</sub> band vibrational frequency was also changed as a consequence of exposure to different light intensity/color. The band position was decreased after the exposure to low lux and again; after exposure to high lux, the band position showed characteristics that depends on the light source wavelength: unchanged with blue-H, decreased for green-H and increased for red-H. Meanwhile, the bandwidth shows two contradictory behavior; it increased after exposure to blue light (low or high lux) and red light (low or high lux) while reduced for green light (low or high lux).

## Discussion

Eye is usually exposed to natural electromagnetic spectrum and man-made visual display devices. Although it has several adapted mechanisms to be protected from light exposure, certain exposure can result in temporal or permanent damage as macular degeneration [4]. Exposing eye to relatively long time-intermittent light has an impact on the cornea. Cornea -as other biological organs- is a membrane bilayer system, and the characteristics of corneal tissue is determined by the properties of this bilayer as the composition of the biopolymers and their interaction to each other as well as the way of packing together. Therefore, variation in any of these characteristics, physiologically will affect the cornea.

Amide A and Amide B bands (asymNH and symNH of protein) are greatly affected due to different wavelengths/lux exposure, while the OH bonds vibrational characteristics of the corneal structure constituents as cholesterol indicated that changes in the microenvironment were takes place. The careful analysis of the decreased vibrational frequency of asymOH and

$\nu_{\text{sym}}\text{OH}$  that were shown in Fig 1 and given in Table 1, indicates that more ordered membrane structure and more vibrational motion are associated with all lux exposure except blue-L.

Deconvolution revealed that the amide I band composed of several underlying bands; the band features in these deconvoluted spectra were different. This indicates that there are changes in the type and relative proportion of the overall protein secondary structures. Low lux exposure from the blue, green or red colors induce marked changes in the corneal protein secondary structure. These light colors were associated with reduced  $\alpha$ -helix and increased  $\beta$ -turns contents with the detection of other protein secondary structural components. Protein insolubility depends on the content of the  $\beta$ -sheet structure; more  $\beta$ -sheet structure resulted in more insoluble protein [9–10]. The decreased  $\alpha$ -helix and increased  $\beta$ -sheet content might indicate either a structural rearrangement of the already existing proteins or expression of new types of proteins that having different structural compositions, and this is clearly observed in corneas after exposure to all lux but blue-L. Our results also indicate that after exposing corneas to blue-H or red-L lux, their protein constituents indicate an increase in both random coil and  $\beta$ -sheets which may give the impetus that protein are denaturated. Accordingly, low lux resulted in more folded (blue-L), insoluble (green-L) and denaturated (red-L) protein while, high lux exposure was associated with more complicated effect represented by the tendency of corneal protein to form aggregate. The red-H exposure led to losing necessary component of the protein secondary structure. The changes in the protein secondary structure were also observed in the fingerprint region (Amide II) as the bending vibrational mode of NH bond was shifted to lower frequency indicates increased random coil formation.

Analysis of the fingerprint region revealed that each color and lux has its own effect on the corneal structure; the variation in the vibrational motion of  $\nu_{\text{sym}}\text{COO}$  vibrational mode—due to amino acid side chain and fatty acids- and  $\nu_{\text{asym}}\text{PO}_2$  one—due to phospholipids and nucleic acids- confirms this last finding where the vibrational motion of the former one was increased for blue-L, decreased for green-L and unchanged for red-L while, for the last one it was unchanged for blue-H, decreased for green-H and increased for red-H. The lower shift in the vibrational frequency of  $\nu_{\text{asym}}\text{PO}_2$  indicates an increase in hydrogen bonding of phospholipids and nucleic acid.

Exposure to different blue, green or red lux was affecting the molecular packing of the acyl chain. The acyl chain packing of the lipid bilayer—i.e. the interaction of hydrocarbon chains with each other—can be monitored by the vibrational frequency of  $\text{CH}_2$  bending mode at  $1461\text{ cm}^{-1}$ . The splitting of this band after exposing the corneas to blue-H and red-H is indicative of an acyl chain orthorhombic or monoclinic crystal system rather than hexagonal one. The change in corneal membrane packing is also evident by the changes noticed in the  $\text{CH}_3$  bending mode.

Molecules can rotate around single bond and in this case are defined as rotamers where, the relative amount of gauche rotamers is indicative of the level of disorder of the bilayer, and it can be calculated using the vibrational frequency of the  $\nu_{\text{asym}}\text{CH}_2$  mode [11–12]. The calculated gauche rotamers percentage was done according to [13], and the interesting finding is that the membrane bilayer of corneas exposed to different color/lux were characterized by higher degree of order; the population of hydrocarbon chain gauche rotamers percentage range is 0.1–0.3 compared to 0.6 in the control corneas.

## Conclusion

The detected microenvironmental changes resulted from exposing the cornea to different colors and/or lux; increased hydrogen bonding, variation in protein secondary structure component as well as variation in the acyl chain packing, were associated with higher degree of membrane bilayer order. These detected changes should have an impact on the corneal structure and its function with a potential possibility of altering its contour; hence vision impairment may results

in. This last probability required further studies to determine which color and intensity may cause the most and the least pronounced changes in the corneal structure.

## Author Contributions

**Conceptualization:** Sherif S. Mahmoud.

**Data curation:** Sherif S. Mahmoud.

**Investigation:** Sherif S. Mahmoud, Wafaa A. Gareeb.

**Methodology:** Sherif S. Mahmoud, Ibrahim H. Ibrahim, Abdel Sattar M. Sallam, Wafaa A. Gareeb.

**Project administration:** Sherif S. Mahmoud.

**Supervision:** Sherif S. Mahmoud, Ibrahim H. Ibrahim, Abdel Sattar M. Sallam.

**Writing – original draft:** Sherif S. Mahmoud.

**Writing – review & editing:** Sherif S. Mahmoud.

## References

1. Jordan DR. The potential damaging effects of light on the eye—part I. *Can. J. Ophthalmol.* 1986; 21(6):216–224. PMID: [3779508](https://pubmed.ncbi.nlm.nih.gov/3779508/)
2. Hayasaka N, LaRue SI, Green CB. Differential Contribution of Rod and Cone Circadian Clocks in Driving Retinal Melatonin Rhythms in *Xenopus*. *PLOS ONE.* 2010; 5(12): e15599. <https://doi.org/10.1371/journal.pone.0015599> PMID: [21187976](https://pubmed.ncbi.nlm.nih.gov/21187976/)
3. Nussbaumer B, Kaminski-Hartenthaler A, Forneris CA, Morgan LC, Sonis HJ, Gaynes BN et al. Light therapy for preventing seasonal affective disorder. *Cochrane Database Syst Rev.* 2015; 8(11): CD011269. <https://doi.org/10.1002/14651858.CD011269>
4. Youssef PN, Sheibani N, Albert DM. Retinal light toxicity. *Eye (Lond).* 2011; 25: 1–14. <https://doi.org/10.1038/eye.2010.149> PMID: [21178995](https://pubmed.ncbi.nlm.nih.gov/21178995/)
5. van Norren D, Voss JJ. Light damage to the retina: an historical approach. *Eye (Lond).* 2106; 30: 169–172. <https://doi.org/10.1038/eye.2015.218> PMID: [26541088](https://pubmed.ncbi.nlm.nih.gov/26541088/)
6. Krimm S, Bandekar J. Vibrational spectroscopy and conformation of peptides, polypeptides, and proteins. *Adv Protein Chem.* 1986; 38(38): 181–364. [https://doi.org/10.1016/S0065-3233\(08\)60528-8](https://doi.org/10.1016/S0065-3233(08)60528-8)
7. Susi H, Byler DM. Resolution-enhanced fourier transform infrared spectroscopy of enzymes. *Methods Enzymol.* 1986; 130: 290–311. [https://doi.org/10.1016/0076-6879\(86\)30015-6](https://doi.org/10.1016/0076-6879(86)30015-6) PMID: [3773736](https://pubmed.ncbi.nlm.nih.gov/3773736/)
8. Surewicz WK, Mantsch HH. New insight into protein secondary structure from resolution-enhanced infrared spectra. *Biochim Biophys Acta.* 1988; 952(2): 115–130. [https://doi.org/10.1016/0167-4838\(88\)90107-0](https://doi.org/10.1016/0167-4838(88)90107-0) PMID: [3276352](https://pubmed.ncbi.nlm.nih.gov/3276352/)
9. Burk MJ, Rougvie MA. Cross- $\beta$  protein structure I: insulin fibrils. *Biochemistry.* 1972; 11:2435–2439. <https://doi.org/10.1021/bi00763a008> PMID: [5040649](https://pubmed.ncbi.nlm.nih.gov/5040649/)
10. Zagroski MG, Barrow CJ. NMR Studies of amyloid beta-peptides: Protein assignments, secondary structure, and mechanism of an alpha-helix-beta-sheet conversion for a homologous, 28-residue N-terminal fragment. *Biochemistry.* 1992; 31(24):5621–5631. <https://doi.org/10.1021/bi00139a028> PMID: [1610809](https://pubmed.ncbi.nlm.nih.gov/1610809/)
11. Allinger NL, Cava MP, de Jongh DC, Johnson CR, Label NA, Stevens CL, editors. *Stereochemistry.* In *Organic Chemistry*, Worth Publishers Inc., 1972, pp. 105–126. <https://doi.org/10.1002/bmb.1973.5690010303>
12. Cameron DG, Casal HL, Gudgin EF, Mantsch HH. The gel phase of dipalmitoyl phosphatidylcholine. An infrared characterization of the acyl chain packing. *Biochim Biophys Acta.* 1980; 596(3):463–467. [https://doi.org/10.1016/0005-2736\(80\)90135-2](https://doi.org/10.1016/0005-2736(80)90135-2) PMID: [6892689](https://pubmed.ncbi.nlm.nih.gov/6892689/)
13. Borchman D, Cecilia MY, Herrell P. Structural characterization of human lens membrane Lipid by infrared spectroscopy. *Invest Ophthalmol Vis Sci.* 1991; 32(8): 2404–2416. PMID: [2071352](https://pubmed.ncbi.nlm.nih.gov/2071352/)